February 2, 2008 hep-ph/0611156

GRAVITON RESONANCES IN $e^+e^- \to \mu^+\mu^-$ AT LINEAR COLLIDERS WITH BEAMSTRAHLUNG & ISR EFFECTS

Rohini M. Godbole[1], *Santosh Kumar Rai*[2], and *Sreerup Raychaudhuri*[3]

Abstract

Electromagnetic radiation emitted by the colliding beams is expected to play an important role at the next generation of high energy e^+e^- linear collider(s). Focusing on the simplest process $e^+e^- \to \mu^+\mu^-$, we show that radiative effects like initial state radiation (ISR) and beamstrahlung can lead to greatly-enhanced signals for resonant graviton modes of the Randall-Sundrum model.

1 Introduction

The next generation of high-energy e^+e^- colliders [1, 2] will necessarily have linear design in order to avoid crippling energy losses from synchrotron radiation. Obviously any linear collider will have single-pass colliding beams, unlike a storage ring where multiple bunch-crossings are possible. High luminosities at linear machines can only be achieved, therefore, by using beams with bunches of high number density — which, in practice, means that the bunches must be focussed to very small sizes. Thus, as compared to a bunch length of around 100 μm at the now-decommissioned LEP Collider, the bunches at the planned TESLA are expected to be around 553 nm $\times$ 5 nm $\times$ 300 nm, while at the CLIC the planned size is 202 nm $\times$ 2.5 nm $\times$ 30 nm. In fact, narrow, intense beams of this kind constitute a basic and unavoidable part of the design of all the proposed high-energy e^+e^- machines including the International Linear Collider (ILC), which is now being planned and designed through a major international effort [3].

Although high number densities per bunch do enable the machine(s) in question to achieve the required luminosity, this feature of the design is not unaccompanied by its own set of problems. These arise because very high densities of charged particles at the interaction point will naturally lead to the generation of strong electromagnetic fields in and around every colliding bunch. Interaction of beam constituents ($e^\pm$) with the (strong) accelerating

[1]Centre for High Energy Physics, Indian Institute of Science, Bangalore 560012, India.
Electronic address: rohini@cts.iisc.ernet.in
[2]Harish-Chandra Research Institute, Chhatnag Road, Jhunsi,-Allahabad 211019, India.
Electronic address: skrai@mri.ernet.in
[3]Department of Physics, Indian Institute of Technology, Kanpur 208016, India.
Electronic address: sreerup@iitk.ac.in

field is well known to generate the so-called *initial state radiation* (ISR), which is essentially a bremsstrahlung phenomenon. At the same time, their interaction with the strong magnetic field generated *by the other beam* will also generate radiation, which goes by the name of *beamstrahlung* [4]. In either case, the effect is to make the initial $e^{\pm}$ radiate one or multiple high energy photons, which not only tend to diminish the beam energy, but can cause further complications by behaving like an extra weak photon beam alongside the electron (positron) one. Thus, precise knowledge of the ISR plus beamstrahlung photon spectrum – and, by inference, of the spectrum of the emitting electron (positron) after photon emission – is essential if we wish to make any realistic predictions at a linear collider.

Fortunately, the spectral distribution of radiated photons can be accurately calculated using only quantum electrodynamics (QED), which may require computation to higher orders of perturbation theory (depending on the desired accuracy), but is eventually extremely precise in its predictions. In fact, over the years, starting with the pioneering work of Weizäcker and Williams [5], more and more refined calculations of the radiated photon spectrum have been developed and most of the recent developments are readily available in the literature[6].

It has long been a part of the folklore of collider physics to consider radiation effects like ISR and beamstrahlung to be a nuisance, insofar as they cause losses in energy and disrupt the beam collimation. This is, in fact, what happens when the machine energy is tuned to a resonance, as, for example, was the case at the LEP-1 collider, which had $\sqrt{s} \simeq M_Z$. At LEP-1, however, because of the low number density per bunch, beamstrahlung effects were negligible. At higher energies, where the beamstrahlung effects are not so weak, radiation-engendered photon beams may, in principle, give rise to a whole new class of backgrounds due to production of lepton pairs [7] and hadrons [8]. Most machine designs, therefore, try to ensure that these radiation effects are minimised — a common trick being to generate *flattened* bunches, which can be shown, other conditions remaining the same, to produce minimum radiation[4]. In this article, however, we pursue the counter-argument that far from being a nuisance, ISR and beamstrahlung can sometimes act as a blessing in disguise, since they are useful in probing new physics scenarios.

Use of radiated photons in new physics studies is by no means a novel idea. Tagging with large-p_T ISR photons has been used in the LEP experiments to search for final states which leave (almost) no visible energy in the detectors – well-known examples being the neutrino counting processes $e^+e^- \to \gamma\nu_\ell\bar{\nu}_\ell$ in the Standard Model, or, in a supersymmetric model, $e^+e^- \to \gamma\tilde{\chi}^0\tilde{\chi}^0$, where the final state is a single photon and missing energy[9]. The hard photon tag has also been used in the study of $e^+e^- \to \gamma\tilde{\chi}^+\tilde{\chi}^-$ with $\tilde{\chi}^\pm$ and the lightest sparticle $\tilde{\chi}^0_1$ being almost degenerate [10], as well as searches for gravitonic states similar

[4]Such beam designs are certainly true of the bunch sizes (mentioned above) at the TESLA and the CLIC.

to the ones under study in this article[11]. For the majority of ISR and beamstrahlung photons, however, the situation is somewhat different, as they are mostly collinear with the beams and hence are simply lost down the beam pipe. Obviously the question of tagging such photons does not arise. However, since each photon carries away a different amount of energy from its parent (radiating) particle, the radiation effects end up in generating an energy distribution of the initially monochromatic electron and positron beams. This energy distribution can be used with profit to search for resonances.

Energy spread of the beams can have a wide variety of consequences. In order to have a focussed discussion, however, we concentrate on one of the simplest and cleanest processes at an e^+e^- collider, viz.

$$e^+\ e^- \to X^* \to \mu^+\ \mu^-$$

where X can be either a massive scalar, vector or tensor particle. In the Standard Model (SM), the only options are $X = \gamma, Z$. For any heavy particle X, there will be resonances in the s-channel process, observable as peaks in the invariant mass $M_{\mu^+\mu^-}$ distribution. At LEP-1, this process, among others, was used to measure the Z-resonance line shape. Heavy particles X predicted in models beyond the Standard Model would show up as similar peaks at a different value of $M_{\mu^+\mu^-}$. These could be, for example, extra Z' bosons or leptophilic scalars, such as the $\widetilde{\nu}_\tau$ in R-parity-violating supersymmetry. In this note, however, we discuss the case where the X are *tensor* particle resonances, the tensors being the massive Kaluza-Klein graviton excitations predicted in the well-known brane-world model of Randall and Sundrum [12][5]

The main motivation of the present study is the fact that it is more or less certain that the next-generation linear collider(s) will be run at a single, or – at best – a limited set of fixed values of the centre-of-mass energy $\sqrt{s}$. For example, in the TESLA studies it has been assumed that the collider will be run at two different values of $\sqrt{s} = 500$ GeV and 800 GeV respectively, the ILC [3] is being planned to run at $\sqrt{s} = 500$ GeV and 1.0 TeV, while the quoted numbers for the CLIC [13] are usually $\sqrt{s} = 1.0$ TeV and 3.0 TeV. However, the massive graviton excitations of the Randall-Sundrum (RS) model, whose masses are not predicted by the theory, may not lie very close to these exact centre-of-mass energy values. In such a case, the contribution due to exchange of RS gravitons will normally be off-resonance and hence strongly suppressed. It may appear, therefore, that a high energy e^+e^- collider will simply miss these new physics effects. However, a spread in beam-energy — such as the one that would be induced by beam radiation — would cause a certain number of the events to take place at an effective (lower) centre-of-mass energy, exciting the resonance(s) and hence providing a significant enhancement in the cross-section. The expected suppression of this cross-section due to one extra power of α is more than compensated by the large

[5]The Randall-Sundrum model is briefly reviewed in Section 3.

resonant cross-section, particularly if the resonances are sharp and narrow. A similar effect, in fact, was observed in Z-resonances at LEP-1.5, running at $\sqrt{s} = 130$ and 136 GeV, and dubbed the 'return to the Z-peak'. Following this idea, therefore, we investigate a 'return to the *graviton* peak(s)' in the process $e^+ e^- \to \mu^+ \mu^-$. This article completes a preliminary study [14] made earlier by the authors, and complements recent studies [15] which investigate similar techniques to identify scalar and vector resonances in other models of new physics.

2 Electron Luminosity with ISR and Beamstrahlung

In the present study, the principal quantity of interest is not the energy of the emitted photons (which are lost down the beam pipe) but the remanent energy of the electron or positron after the photon emission. This is because the photon is lost down the beam pipe, but the effective centre-of-mass energy of the e^+e^- system (and hence of the final states barring the lost photon(s)) will be determined by this reduced beam energy. Noting that there may be single or multiple photon emission due to both ISR and beamstrahlung effects, a convenient way to obtain an energy spectrum for the electron (positron) is to make use of the *structure function formalism*, which has hitherto been used mainly to predict excess Standard Model backgrounds[7, 16]. In this method – which is inspired by and closely follows the standard techniques developed for hadronic interactions – the scattering cross section for a given process

$$e^+(p_1) + e^-(p_2) \to F(x_1 p_1 + x_2 p_2) + (\gamma)$$

where F is any (observable) final state, is given by

$$\sigma[e^+e^- \to F(\gamma)] = \int dx_1 dx_2 \; f_{e/e}(x_1) \; f_{e/e}(x_2) \; \hat{\sigma}[e^+e^- \to F](\hat{s}) \; , \tag{1}$$

where, as in the case of hadron colliders, x is the momentum fraction of the electron (positron) in the initial state while the *electron luminosity* function $f_{e/e}(x)$ describes the probability of a beam electron of energy $E_b = \sqrt{s}$ emitting one or more photons of total energy $(1-x)E_b$, thereby degrading its own energy to $E_e \; = \; xE_b$. It is now a simple matter to show that for colliding beams the effective centre-of-mass energy will be $\sqrt{\hat{s}} \simeq \sqrt{x_1 x_2 s}$. The final state, in our study, is $F = \mu^+\mu^-$.

The electron luminosity function $f_{e/e}(x)$, introduced above, must include both the ISR and beamstrahlung effects. The ISR contribution is usually calculated in terms of the momentum fraction x using a Weizäcker-Williams approximation, which is perturbatively corrected to take into account emission of multiple soft photons. The result, to one-loop order[6] is given in terms of a normalised distribution function [18]

$$f^{\rm ISR}_{e/e}(x) = \frac{\beta}{16}\left[(8+3\beta)(1-x)^{\beta/2-1} - 4(1+x)\right] \; , \tag{2}$$

[6] which is free of collinear divergences, á-la Bloch and Nordsieck [17]

where the β-parameter is

$$\beta = \frac{2\alpha}{\pi}\left(\log\frac{s}{m_e^2} - 1\right) \ , \tag{3}$$

and α denotes the running fine-structure constant evaluated at the beam energy E_b. At linear collider energies, β varies more-or-less between 0.13—0.15, indicating that the first term in Eqn. (2) has a negative exponent. This makes the function $f_{e/e}^{\rm ISR}(x)$ rise steeply as $x \to 1$. Of course, there is no singularity at $x = 1$ because the overall function is normalised, but nevertheless, this steep increase ensures that the bulk of the electron luminosity lies above $x > 0.9$. This immediately tells us that ISR is a rather weak effect insofar as spreading out the beam energy is concerned. A glance at the dotted line (marked ISR) in Figure 1 makes this amply clear. Consideration of ISR effects alone will not, therefore, be of much use in exciting a resonance, unless the latter happens to lie very close to the machine energy (as was the case with the Z-resonance at LEP-1.5).

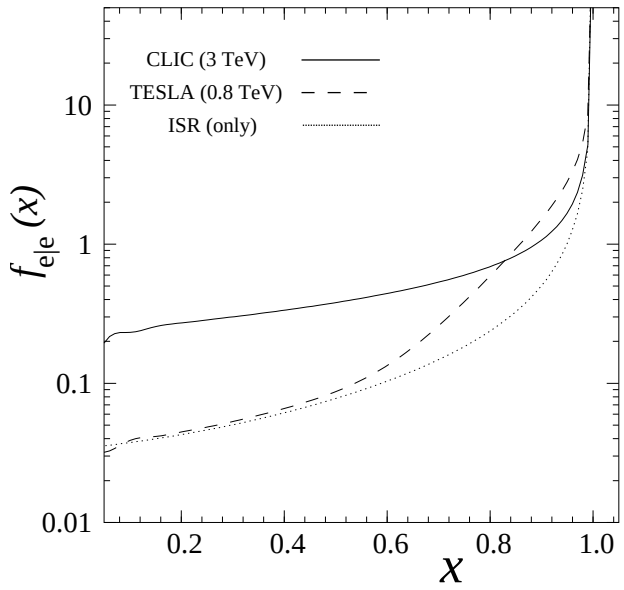

Figure 1: *Illustrating the electron luminosity $f_{e|e}(x)$ as a function of $x = E_e/E_b$, the energy fraction of the electron (positron) after radiation of one or more photons. The (dashed) solid line shows the prediction at the* TESLA (CLIC) *machine, where the beamstrahlung parameter is $\Upsilon = 0.09$ (8.1). The dotted line shows the (unconvoluted) ISR prediction at the* TESLA *energy.*

This situation changes quite spectacularly when we incorporate beamstrahlung effects. Unlike the ISR spectrum, the beamstrahlung spectrum depends not only on the electron beam energy E_b and the remanent momentum fraction x, but also on such highly machine-specific parameters as the bunch length σ_z and the beamstrahlung parameter Υ. The latter, a measure of the effective magnetic field of the bunches, is given by

$$\Upsilon = \frac{E_b}{m_e}\left(\frac{B}{B_c}\right) \ , \tag{4}$$

where B is the effective magnetic field strength in the beam, and $B_c = m_e^2/e\hbar \simeq 4.4 \times 10^{13}$ Gauss is the Schwinger critical field for electrons. The magnetic field B will be determined by the density of electrons (positrons) in the colliding bunches. For beams with a Gaussian energy profile, the effective or mean value of Υ is, thus, given by [19]

$$\Upsilon = \left(\frac{5r_e^2}{6\alpha m_e}\right) \frac{E_b N_e}{\sigma_z(\sigma_x + \sigma_y)} \tag{5}$$

where N_e is the number of electrons or positrons in a bunch, σ_x, σ_y are the transverse bunch sizes, and $r_e \simeq 2.818 \times 10^{-13}$ cm is the classical electron radius. It may be noted that the effective beam sizes $\sigma_x, \sigma_y, \sigma_z$ which appear in the above equation are slightly different from the nominal beam sizes (created by focussing magnets) because of the so-called beam disruption effect, i.e. the tendency of the beams to deform in the strong electromagnetic fields experienced just before (and during) the collision process. In terms of these parameters, then, the beamstrahlung spectrum for radiated photons can be written [19] in terms of the momentum fraction x, as

$$f_{\gamma|e}^{\rm beam}(x) \;=\; \frac{\kappa^{1/3}}{\Gamma(\frac{1}{3})} \frac{e^{-\kappa x/(1-x)}}{\{x^2(1-x)\}^{1/3}} \left[\frac{1-\omega}{\tilde{g}(x)} \left\{1 - \frac{1-e^{-N_\gamma \tilde{g}(x)}}{\tilde{g}(x) N_\gamma}\right\} + \omega \left\{1 - \frac{1-e^{-N_\gamma}}{N_\gamma}\right\}\right], \tag{6}$$

with

$$\tilde{g}(x) = 1 - \frac{1}{2}(1-x)^{2/3}\left[1 - x + (1+x)\sqrt{1+\Upsilon^{2/3}}\right] \;, \qquad \kappa = \frac{2}{3\Upsilon} \;, \qquad \omega = \frac{1}{6\sqrt{\kappa}} \;. \tag{7}$$

Here, $\Gamma(\frac{1}{3})$ is the usual Euler gamma function and the quantity N_γ, denoting the average number of photons emitted per electron, is given by

$$N_\gamma = \left(\frac{5\alpha^2 m_e}{2r_e}\right)\left(\frac{\sigma_z}{E_b}\right) \frac{\Upsilon}{\sqrt{1+\Upsilon^{2/3}}} \;, \tag{8}$$

If we were to consider only single photon emission, the electron spectrum — which is what we actually require — would be just complementary to the photon spectrum in Eqn. (6) for $N_\gamma = 1$. However, we also need to take into account multiple photon emissions [7, 19, 6]. This calculation is obviously much more involved, but for our purposes it suffices to use a closed-form approximation for the function $f_{e/e}^{\rm beam}(x)$, viz.,

$$N_\gamma f_{e/e}^{\rm beam}(x) = (1-e^{-N_\gamma})\delta(1-x) + \frac{e^{-\eta(x)}}{1-x} \sum_{n=1}^{\infty} \left\{1 - x + x\sqrt{1+\Upsilon^{2/3}}\right\}^n \frac{\eta(x)^{n/3}\gamma_{n+1}(N_\gamma)}{n!\;\; \Gamma(\frac{n}{3})} \tag{9}$$

where $\eta(x) = \kappa(\frac{1}{x} - 1)$, and $\gamma_a(s)$ is the incomplete $\gamma-$function, defined by

$$\gamma_a(x) = \int_0^a dt\; t^{x+1} e^{-t} \;.$$

The expression in Eqn. (9) is quite accurate for low values of Υ up to about $\Upsilon \approx 10$, but becomes increasingly inaccurate above this value[7].

Taking both ISR and beamstrahlung effects into account, and assuming that they take place in quick succession, the electron spectrum at the collision point can be well approximated by a simple convolution of the two respective spectral densities [7, 16]:

$$f_{e|e}(x) = \int_x^1 \frac{d\xi}{\xi} \, f_{e|e}^{\rm ISR}(\xi) \, f_{e|e}^{\rm beam}(\frac{x}{\xi}) \, . \tag{10}$$

This formula can now be used to generate the spectrum illustrated in Figure 1, which shows the (convoluted) electron luminosity for the given design parameters at the TESLA, running at $\sqrt{s} = 800$ GeV (dashed lines) and at the CLIC, running at $\sqrt{s} = 3.0$ TeV (solid lines). The pure ISR spectrum at TESLA energy, which has already been remarked upon, is also shown for purposes of comparison (dotted lines). Noting that the ordinate in this plot is logarithmic, it is immediately apparent that beamstrahlung effects serve to broaden the energy spectrum of the electron much more significantly than ISR alone. This energy spread may, therefore, be used, as explained in the previous section, to excite resonances quite some way away from the machine energy.

To get quantitative results, we now require to substitute the function $f_{e|e}(x)$ as obtained from Eqn. (10) into the general formula in Eqn. (1) to get the final cross-section. Resonances, if any, will then be predicted at the appropriate values of $\hat{s} = x_1 x_2 s$. The remaining part of this article discusses how this can happen, and what our expectations in respect of new physics – specifically massive RS gravitons – should be.

3 Graviton Resonances

The two-brane model of Randall and Sundrum (RS) has one extra dimension compactified on a $\mathbf{S}^1/\mathbf{Z}_2$ orbifold, and two (four-dimensional) 3-branes at the orbifold fixed points. It also assumes finely-tuned cosmological constants on the two branes and in the intervening space or 'bulk'. On one of these 3-branes, which is identified with the observed Universe, we have an effective theory where the SM is augmented by a set of Kaluza-Klein excitations of the graviton. These behave like massive spin-2 fields with masses $M_n = x_n m_0$, where the x_n are the zeroes of the Bessel function of order unity, n is a non-negative integer and m_0 is an unknown mass scale close to the electroweak scale, which can be related to the radius of compactification R_c and the curvature parameter $\mathcal{K}$ of the orbifold $\mathbf{S}^1/\mathbf{Z}_2$, through the expression

$$m_0 = \mathcal{K} e^{-\pi \mathcal{K} R_c} \tag{11}$$

where R_c is the compactification radius of the orbifold and $e^{-\pi \mathcal{K} R_c}$ is the famous exponential 'warp factor' of the RS model. We treat m_0 as one of the free parameters of the model.

Current experimental data from the Drell-Yan process at the Tevatron constrain m_0 to be more-or-less above 160 GeV [20].

The other undetermined parameter of the theory is the curvature of the fifth dimension expressed as a fraction of Planck mass and is given by $c_0 = \mathcal{K}/M_P$. Feynman rules for the Randall-Sundrum graviton excitations can then be read off from the well-known Feynman rules for the large extra dimension model given in Ref.[21] by making the simple substitution $\kappa \to 4\sqrt{2}\pi c_0/m_0$. Noting that the massive graviton states exchanged in the s-channel can lead to Breit-Wigner resonances, a long but straightforward calculation must be undertaken to find the cross-section for the process $e^+\ e^- \to \mu^+\ \mu^-$. We have performed this calculation and incorporated our results in a simple Monte Carlo event generator to get numerical estimates.

For our numerical analysis we have chosen the parameters of the RS model to be $m_0 = 170$ GeV and $c_0 = 0.01$, which implies that the lightest ($n = 1$) massive excitation has mass $M_1 \simeq 652$ GeV, placing it just beyond the present detection reach of Run-2 data at the Tevatron [20]. With this choice, however, the next excitation is predicted to have mass $M_2 > 1$ TeV, which would put it well beyond the kinematic reach of an 800 GeV machine. At the TESLA or even the ILC, therefore, we expect to detect one – and only one – resonance. The value of c_0 has initially been chosen at the lower end of the possible range, since this leads to a longer lifetime for the Kaluza-Klein state and hence a sharper resonance in the cross-section. It also enables us to evade the more stringent bounds from the Tevatron which arise for higher values of c_0. The effects of varying c_0 are shown in a later section.

We have run the event generator for the cross section subject to the following kinematic cuts on each of the final state muons:

- transverse momenta: $p_T^{\mu^\pm} > 20$ GeV
- scattering angle: $10^0 < \theta_{\mu^\pm} < 170^0$.

These are almost standard acceptance cuts and are known to eliminate most of the backgrounds from beam-beam interactions as well as two-photon processes. Some of our results are illustrated in Figure 2, which shows the bin-wise distribution of invariant mass $M_{\mu^+\mu^-}$ of the (observable) final state at the TESLA running at $\sqrt{s} = 800$ GeV. In Figure 2(a), we have plotted the distribution predicted in the SM. Figure 2(b) shows the *excess* over the SM prediction expected in the Randall-Sundrum model and Figure 2(c) shows the signal-to-background ratio.

At a linear collider with a fixed center-of-mass energy (i.e. no radiation effects), all the events should be concentrated in a single invariant mass bin at $M_{\mu^+\mu^-} = \sqrt{s}$. In Figure 2 this corresponds to the solid vertical bar at the right edge of the $M_{\mu^+\mu^-}$ distribution. Comparison

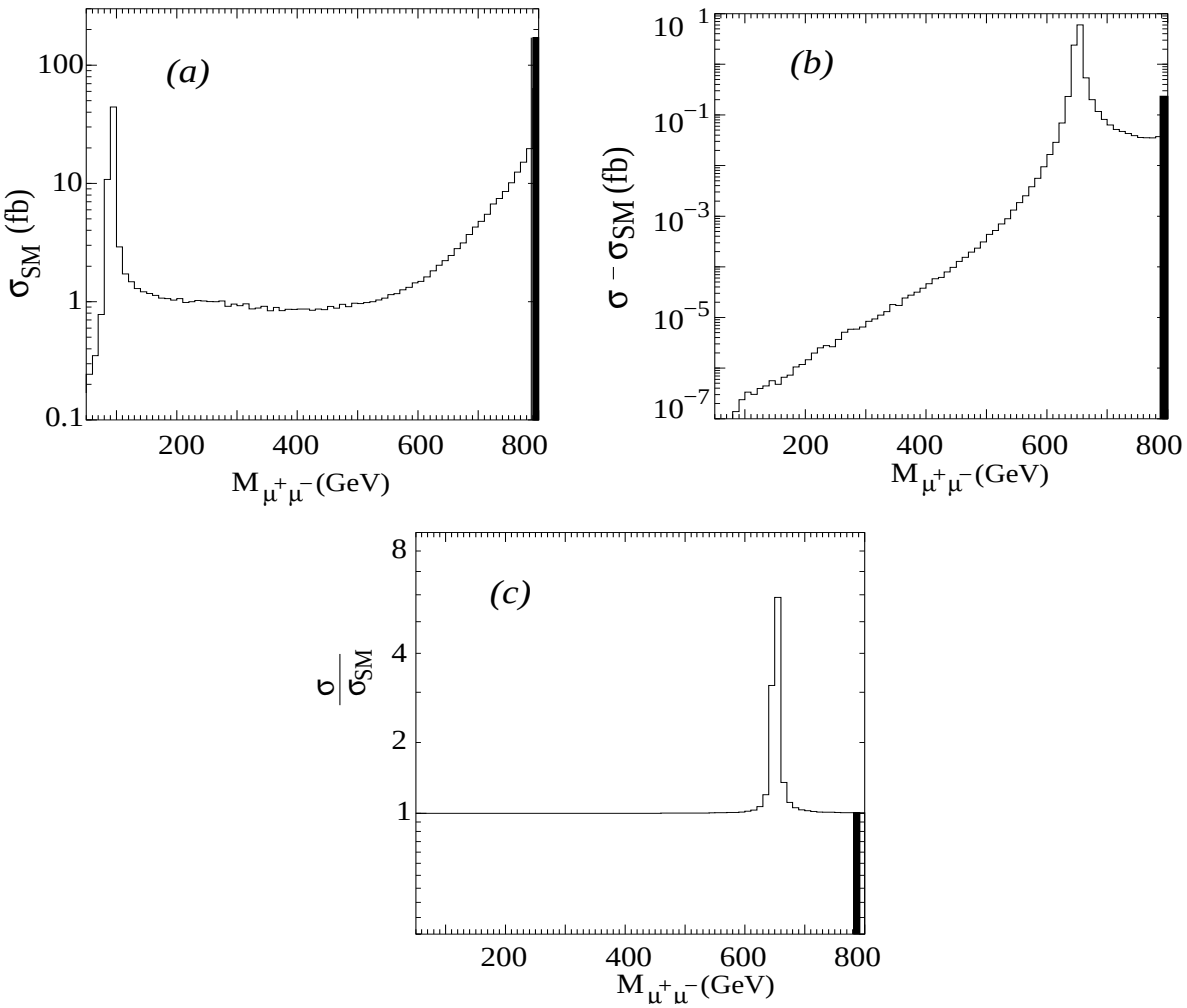

Figure 2: *Invariant dimuon mass distribution with (histogram) and without (solid vertical bar) radiative effects. The figures correspond to* (a) *the bin-wise cross-section σ_{SM} for the SM background,* (b) *the bin-wise excess cross-section $(\sigma - \sigma_{SM})$ for the RS contribution alone and* (c) *the signal-to-background ratio σ/σ_{SM}. 'Bin-wise' cross-sections refer to integrated cross-sections in each bin of $M_{\mu^+\mu^-}$.*

of Figures 2(a) and 2(b) — which are plotted on vastly differing scales — show that in this 'ideal' case, the expected signal is very small indeed, about 1 in 10^4. Naturally the ratio indicated by the solid bar in Figure 2(c) is almost precisely unity. This is not surprising, since our parameter choice leads to a graviton of mass around 652 GeV and decay width of a few GeV, which means that the resonance lies many decay widths away from the collision energy $\sqrt{s} = 800$ GeV.

The situation is not so bad, however, as the solid bars would seem to indicate. This is, in fact, the main thrust of our work. The histograms in Figure 2 show the invariant mass distribution *when radiative effects are included*. It is immediately apparent that the effective centre-of-mass energy $\sqrt{\hat{s}} = M_{\mu^+\mu^-}$ is spread out from the beam energy $\sqrt{s}$. In (a), where only the SM prediction is plotted, we can see a distinct peak at the lower end which showcases the 'return

to the Z-peak'. The cross-section for this peak is not as high as has been seen at LEP and SLD in the case of a narrow Z resonance, since in the present case the peak corresponds to very small values of the energy fraction x of the electron ($x \simeq 0.11$), for which the electron luminosity is extremely small ($f_{e|e}(x) \simeq 0.035$), as can be seen from Fig. 1. Nevertheless, it may be seen that the peak is still higher than the cross-section at the design energy $\sqrt{s}$.

Since there are no other massive resonances in the SM, the shape of the rest of the histogram in Fig. 2(a) simply reproduces the electron luminosity curve shown in Figure 1. In Fig. 2(b), however, where the RS model predictions are considered, the radiative return to a resonant 652 GeV Kaluza-Klein mode of the graviton is quite apparent. This resonance lies much closer to the machine energy, and hence is excited for a much larger value of energy fraction ($x \simeq 0.82$), where the electron luminosity ($f_{e|e}(x) \simeq 0.3$) is significantly larger. It may be pointed out that the scales along the ordinate are quite different in Fig. 2(a) and 2(b), showing that the graviton peak is roughly an order of magnitude smaller than the Z peak, despite the larger electron flux. The histogram in Fig. 2(c), shows the signal-to-background ratio. This ratio removes the Z-peak and throws the graviton resonance into prominence, presenting us with a clear signal for a new resonant particle.

It is important to note that although we have concentrated on a massive graviton resonance, the above analysis requires only the existence of a (neutral) resonant particle, with mass in the relevant energy range and coupling to both e^+e^- and $\mu^+\mu^-$ pairs. Thus, the same technique may be used effectively to study

- extra Z' bosons arising in models with extended gauge symmetries [22];
- Kaluza-Klein excitations of Z-boson in models with universal extra dimensions[23] ;
- leptophilic scalars, such as dileptons and the sneutrinos of R-parity violating supersymmetry with LLE-type operators[24].

All of the above theories would predict similar resonances. If, indeed, such an effect is seen, the question would at once arise as to the nature — especially the spin — of the resonant (bosonic) particle. For example, only the confirmation of two units of spin would establish the existence of a massive graviton resonance. This question is taken up in the next section.

Before concluding the present section, we briefly discuss an important issue, especially from the point of view of the experimentalist, viz. the choice of a $\mu^+\mu^-$ final state. This is well known to be one of the cleanest signals, but – especially for gravitons – this channel is suppressed by the low branching ratio for $G_n \to \mu^+\mu^-$ compared with the branching ratio to a pair of hadronic jets, i.e. $G_n \to q\bar{q}$ or gg. However, in looking for resonances in two-jet final states we must remember that two-photon processes can give rise to a substantial dijet

production rate for invariant masses quite a bit smaller than the nominal centre-of-mass energy $\sqrt{s}$ of the collider [8, 16]. This would heavily contaminate the signal and may render the results inconclusive. This argument applies for $\tau^+\tau^-$ final states as well, since the $\tau^\pm$ decay to (narrow) jets. The e^+e^- final state will have a large contribution from the t-channel exchanges in Bhabha scattering, against which background the feeble signal may be totally lost. A similar argument holds for the ZZ final state, which can be nicely reconstructed from the leptonic decays of the Z, but is heavily contaminated by Z pair production from t-channel electron exchange diagrams. It turns out, therefore, that the $\mu^+\mu^-$ channel chosen in the present work is indeed the best one to trigger on in spite of the large suppression caused by the low branching ratio.

4 Identifying Resonant Particles

In the previous section we have demonstrated how radiative effects like ISR and beamstrahlung could be effectively utilised to highlight a resonance in e^+e^- annihilation. Specifically, we showed that for a RS graviton with a mass which is accessible kinematically, one would see a distinct peak in the invariant mass distribution of the $\mu^+\mu^-$ pair in the final state. However, merely identifying a resonance — even if the width can be measured and is found to fit the theory — does not automatically indicate whether we have seen a spin-2 particle, for it could very well be an exotic vector or scalar particle (of the types listed above, or even of completely unknown type) of the same mass and comparable decay width. One requires, therefore, to make some extra measurements to identify the nature of the resonance.

One of the important features which distinguishes a graviton resonance from most of the vector or scalar resonances is the fact that it has, for the same mass and couplings of comparable strength, a greater decay width. This is essentially because the graviton couples to all particles with a coupling strength which is determined only by the spacetime quantum numbers and is blind to all the internal quantum numbers, i.e. the massive graviton can decay into *any* pair of particles, so long as it is kinematically possible. The presence of more channels thus enhances the decay width, even when the overall coupling is the same as those in the case of other resonances. We may, therefore try to identify *broad resonances* as a distinctive feature of RS graviton resonances.

To make a detailed analysis, we consider, as before, the process $e^+\ e^- \to X^* \to \mu^+\ \mu^-$ where X can be, respectively, a generic spin-0 (scalar) particle or a spin-1 (vector) particle or a RS graviton *of the same mass*. We chose a fixed mass of 600 GeV for all the above particles and, in every case, ran an event generator with the same kinematic cuts as above. The cross-sections vary for the different exchange particles, depending on the strength of interactions and the width of the decaying particle. We have, therefore, taken values for the couplings

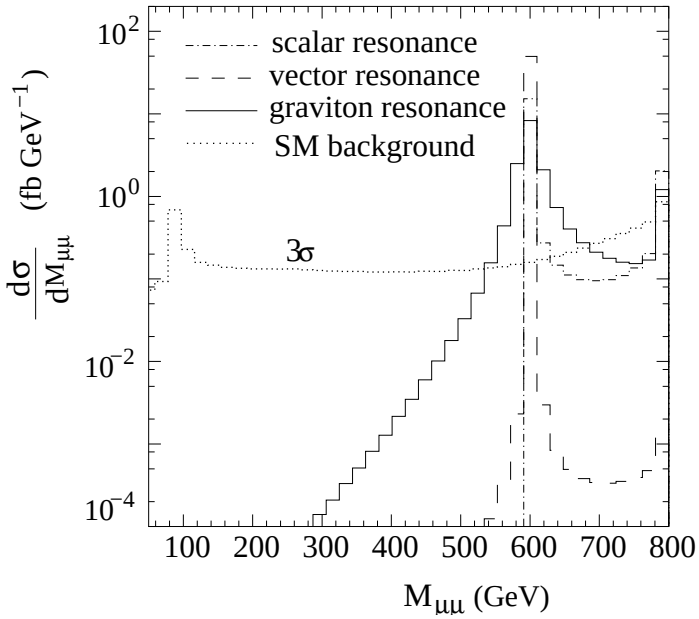

Figure 3: *Bin-wise invariant $\mu^-\mu^-$ mass distribution for, respectively, scalar (dash-dot line), vector (dashed line) and RS graviton (solid line) resonances of similar mass and* total *cross-section. Radiation effects are included, and the dotted histogram indicates the 3σ SM background.*

which, while remaining consistent with present experimental bounds[25] for the given mass, are chosen such that the *total* cross-sections for the different cases (spin-0, spin-1 and spin-2) are all equal. In Figure 3 we show the bin-wise distribution of invariant mass $M_{\mu^+\mu^-}$ of the (observable) final state for the different cases. Figure 3 is thus similar to Figure 2(b), except that all three types of particles are included instead of just RS gravitons. A glance at the figure shows that there is indeed a significant difference in the decay width, with the scalar resonance being very narrow and the graviton resonance being much broader. We note, however, that it is the excess signal over the SM background that is of significance and in this case, the background is quite large. In fact, if we plot the 3σ fluctuation in the SM with 500 fb^{-1} luminosity, it is seen that only the tip of the resonance peaks would show up, and it is likely, therefore to be very difficult to distinguish between these little bumps over the SM background, considering that there would be large error bars in the experimental data.

A more direct measurement aimed at identifying the spin of the resonant particle is to plot the angular distribution of the final state particles, since it is well known that the spin of the decaying resonance leaves a distinct imprint on this angular distribution. However, we must note that the e^+ and e^- no longer collide in the centre-of-mass frame because of radiation effects. It may seem, on first thoughts, that the resultant boost will not be so significant for collisions at 800 GeV if a 652 GeV resonance is produced, but this is not, in fact, the case. To show that the collision does, in fact, take place in a highly-boosted frame, we have plotted the distribution for the opening angle $\theta_{\mu\mu}$ of the final state muons in Figure 4.

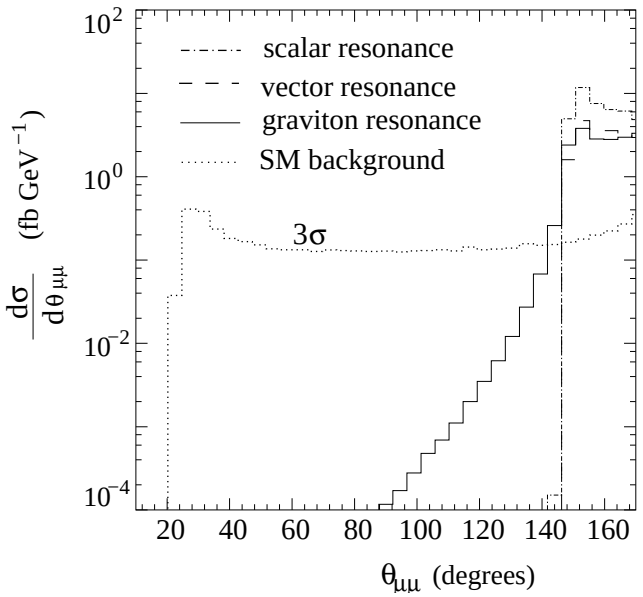

Figure 4: *Bin-wise opening angle distribution for the final state $\mu^+\mu^-$ pair, for scalar, vector and RS graviton resonances of similar Mass and total resonant cross-section. The conventions followed are the same as in Figure 3.*

In the absence of radiation effects one would expect the muons to scatter back-to-back. i.e. $\theta_{\mu\mu} = 180^o$. However, the energy carried away by radiated photons makes the final state $\mu^+\mu^-$ pair scatter at different angles so that the *overall* four-momentum is conserved. Figure 4 clearly shows that this effect is not only significant, but dominates the much weaker differences due to spin, rendering the three histograms for, respectively, scalar (dot-dash), vector (dashed) and RS gravitons (solid) quite indistinguishable. As in Figure 3, the long tail of the distribution in the RS case is quite lost in the SM background, even at the 3σ level.

All is not lost, however, for we can still reconstruct the angular distribution of the muons *in the rest frame of the decaying particle*. To achieve this, we simply calculate the longitudinal component of the total momentum of the two muons $p_L^+ + p_L^-$ and use it to compute the boost experienced by their parent particle X with respect to the laboratory frame. We then boost back the decay products (muons) to the rest frame of X and plot the muon angular distribution in this reconstructed rest frame. Figure 5 shows this (normalised) angular distribution, where θ^* is the angle of the final state μ with respect to the boost axis. The scalar (dot-dash), vector (dashed) and RS graviton (solid) distributions are now quite different, with the curves in Figure 5 representing the first three Legendre polynomials in $\cos\theta^*$, which is expected in view of the appropriate angular momentum representations. The dips in the cross-section for a scalar resonance at the extreme values $\cos\theta^* = \pm 1$ are artifacts of the kinematic cuts mentioned in Section 3. Though we have not shown it explicitly in the figure, we estimate that the typical error bars expected for 500 fb^{-1} luminosity should be small enough to enable the three cases to be clearly distinguished. This reconstruction

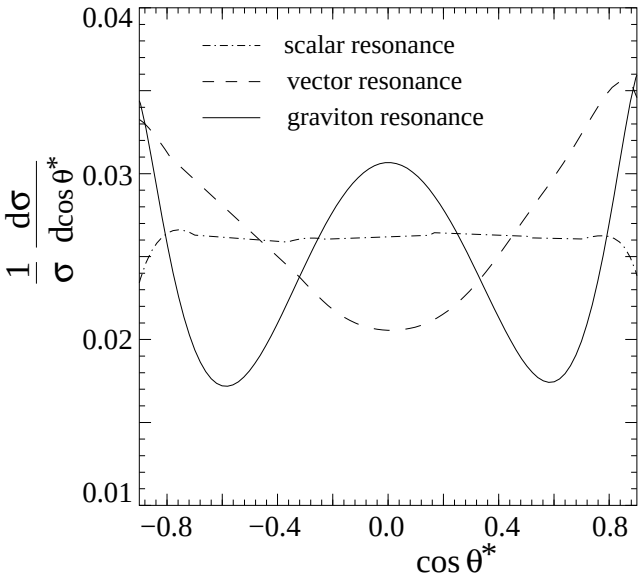

Figure 5: *The angular distribution of the final state muon in the rest frame of the decaying particle with respect to the boost axis, where the boost is due to radiated photons, for scalar, vector and RS graviton resonances respectively. The line styles are the same as in the previous two figures, but the ordinate shows the normalised differential cross-section rather than the bin-wise cross-section.*

technique is, therefore, fairly powerful and can be used to identify the spin of the resonant particle quite unambiguously.

One obvious spoiler for the above technique would be a situation where there are *two* or more particles with the same mass but different spin. Though this is quite unlikely in most extensions of the SM, it is far from impossible in universal extra dimensions models[7], where the tree-level masses of the Kaluza-Klein excitations of all SM particles are determined by the size of the extra dimension. Fortunately, the only resonances which can be excited in e^+e^- collisions in this model are vector-like (excitations of the photon and the Z), so their presence would pose no problems for graviton identification.

5 Higher Energies and Luminosities

Apart from the spin, the other really distinguishing feature of Kaluza-Klein excitations is the fact that there exists a tower of such states with successively increasing mass. The observation of such multiple spin-2 excitations would be a clear indication of a theory with extra dimensions. In the case of the RS model, we know that these masses vary as the zeros x_i of Bessel functions of order unity, which means that the first three resonances satisfy the ratio

$$M_1 : M_2 : M_3 \approx 1 : 1.83 : 2.65 \ . \tag{12}$$

[7] which are similar and closely related to, but distinct from, the RS model[26]

If one could, for example, detect three resonances and establish that their mass ratio satisfies this condition, we would have gone a long way toward establishing the truth of the RS model. It, is, therefore, important to detect more of the graviton resonances, apart from the lightest one which has been the subject of most of the preceding discussions.

It is practically a theorem in high energy physics that increase in the machine energy and/or the luminosity automatically results in an increase in the power of the machine to search for new physics. This is very much applicable to the search for resonances. In the present case, if we consider the RS model with $m_0 = 170$ GeV, we have already seen that the first graviton resonance at about 652 GeV is all that is accessible at a 800 GeV machine. At the 500 GeV option of the ILC, the possibility of exciting RS graviton resonances is already ruled out by the Tevatron data. The next two resonances, for $m_0 = 170$ GeV, lie at around 1193 GeV and 1727 GeV respectively, and would be even higher if m_0 is higher. We see, therefore, that the higher graviton resonances are fairly heavy and can be excited only at a machine running at a significantly higher energy.

Of all the e^+e^- machines of linear collider type proposed, the CLIC, running at $\sqrt{s} = 3$ TeV would be the most likely one where these higher graviton resonances may be seen. In fact, one of the positive features (so far as this analysis is concerned) of the CLIC is that radiation effects are considerably enhanced, the beamstrahlung parameter being as high as $\Upsilon = 8.1$ for the CLIC design parameters at $\sqrt{s} = 3$ TeV. This, is turn, would cause a much larger energy spread when compared with the TESLA prediction (see Figure 1). We make use of this fact and illustrate in Figure 6 how the multiple resonances in the RS model could be excited at the CLIC[8]. Figure 6 clearly shows three resonances, with a hint of a fourth. If the qualitative features of this prediction are reproduced by the actual data, it will have to be followed up by two checks, namely (a) that the successive peaks are in the ratio $1 : 1.83 : 2.65$, and (b) that the events concentrated around each of the peaks follow the spin-2 angular distribution illustrated in Fig. 5. If *all* of these are confirmed, we can claim a 'smoking gun' signal for the RS Model. If no such effects are seen, the RS model is disfavoured but not ruled out, since it would simply mean that the lower bound on m_0 moves up to around 780 GeV in place of the present lower bound of around 160 GeV. If *some* of these predictions are confirmed and others are not, it would be a challenge to the high energy physics community to find a reasonable explanation, and it is quite possible that in any such explanation extra dimensions will play an important role.

It could be the case, as mentioned above, that $m_0 > 780$ GeV and hence graviton excitations are too massive to be accessed even at the CLIC. In fact, as the graviton mass scale m_0

[8]In our numerical analysis the kinematic cuts were kept identical with those imposed at $\sqrt{s} = 800$ GeV, a feature which may need reconsideration in a more realistic study. It suffices, however, for our purposes here, which are chiefly illustrative, to keep the same kinematic cuts.

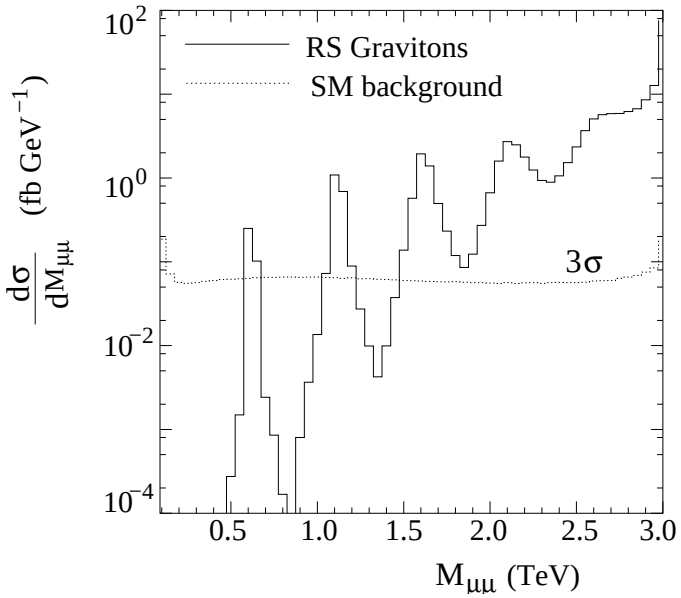

Figure 6: *The invariant mass $M_{\mu^+\mu^-}$ distribution at the CLIC collider running at $\sqrt{s} = 3$ TeV for RS graviton resonances (solid line). As in Fig. 2, the RS model parameters are chosen to be $m_0 = 170$ GeV and $c_0 = 0.01$. The dotted histogram shows, as in the preceding figures, the 3σ SM background.*

increases, the peaks in Figure 6 shift to the right of the graph and eventually move out of the energy reach of the machine. It is also possible that the graviton resonance peaks become too broad to be identified as such. It is, thus, a relevant question to ask how far the parameter space can be probed at the design energies and luminosities. To take up this question, we set up as a discovery paradigm the situation when the invariant mass distribution shows a significant deviation from the SM prediction. To quantify this, we calculate a bin-wise-summed variance χ^2 in the $M_{\mu\mu}$ distribution

$$\chi^2(m_0, c_0) = \sum_i \frac{\left(N_i^{(SM+RS)} - N_i^{(SM)}\right)^2}{N_i^{(SM)}} = \mathcal{L} \sum_i \frac{\left(\sigma_i^{(SM+RS)} - \sigma_i^{(SM)}\right)^2}{\sigma_i^{(SM)}} \tag{13}$$

where $\mathcal{L}$ is the integrated luminosity, N_i denotes the number of events in a bin and σ_i is the cross-section in that bin. In the denominator, we take only the Gaussian errors and neglect systematic effects (which are completely unknown at this early stage in linear collider development). To observe a deviation at 95% confidence level, we require this $\chi^2(m_0, c_0)$ to be greater than a fixed number, which is, for example, 23.46 for 20 bins in $M_{\mu\mu}$. We may, therefore, map out the entire m_0–c_0 plane for different energies and luminosities, calculating the radiation effects in each case using the design beam parameters given in the literature. Our results are shown in Figure 7, where the regions to the left of and above the curves correspond to an observable effect. For comparison, the current bounds from the Tevatron Run-2 data are also given as a shaded region, with the unshaded region indicated at the lower left corner being an extrapolation from the published result. It is clear from the graph that the TESLA, running at 800 GeV, can only improve on the Tevatron bounds marginally,

that too for the high luminosity option, increasing the discovery reach by about 150 GeV. This is quite as one might expect, given that the mass of the lightest graviton is already known to lie above 600 GeV. The CLIC, on the other hand, will improve the discovery reach greatly, as the wide regions to the left of the corresponding curves indicate.

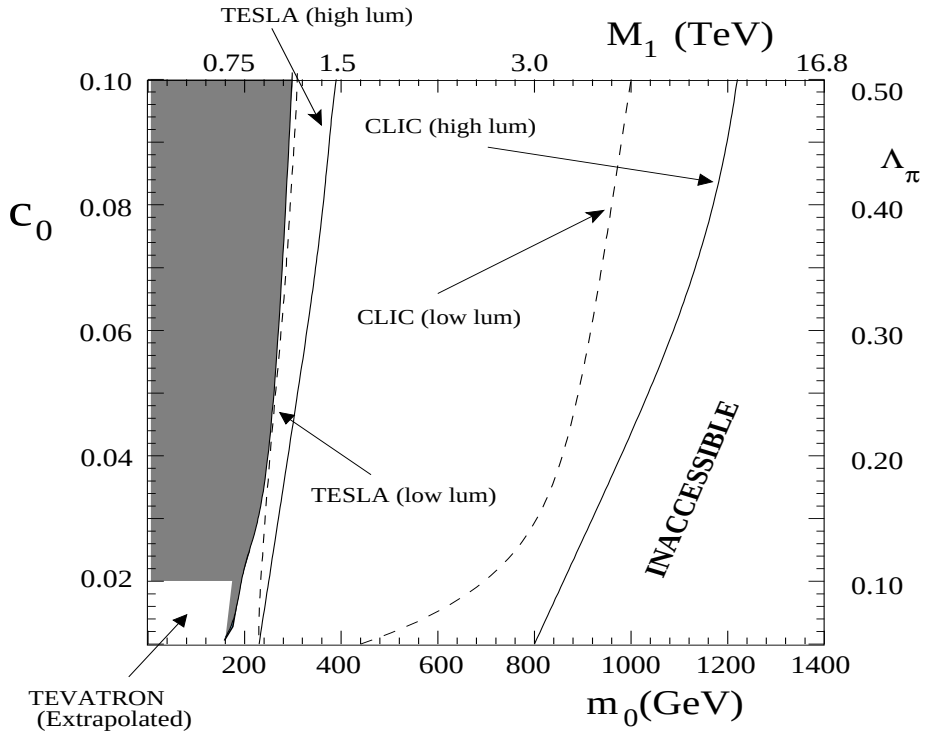

Figure 7: *Discovery limits in the c_0–m_0 plane for RS gravitons at different machines, assuming different centre-of-mass energies and integrated luminosities. Regions to the right of the curves are inaccessible to the machine in question. The dark shading represents the Tevatron bound from Run-2 data, with the small unshaded region at the bottom representing an extrapolation from the published bounds (which go down to only $c_0 \simeq 0.02$). The dashed lines represent the regions accessible to TESLA and CLIC in the low luminosity options, while the solid lines represent the corresponding high luminosity options. The scales marked on the upper and right margins of the graph represent the alternative parametrization in terms of M_1 and Λ_π which are also found in the literature.*

We have deliberately avoided showing possible LHC bounds in Figure 7. At the LHC, such bounds would arise from the combined study of a whole set of different processes, most of which have been investigated separately in the literature in detail. However, these analyses use different assumptions about the luminosity and detection efficiency and even employ theoretical formulations of some of the tricky issues in the calculations (such as the handling of transPlanckian events). Until a consolidated study is available in the literature, which takes the union of all the accessible regions[9], therefore, it does not seem very meaningful to put LHC discovery limits in the graph. However, a qualitative statement (perhaps more

[9]like the studies available for the supersymmetric Higgs parameter space, for example.

of an educated guess) is definitely in order: the LHC discovery limits will definitely better those of the TESLA and the ILC and may be comparable with those possible at the lower luminosity option of the CLIC, especially for lower values of c_0 where the resonances are sharp. The boundaries of the accessible region will probably be differently shaped from the ones shown for linear colliders, with the LHC performance being worse for large c_0, where the resonances are broad. More than this, one cannot say without performing a consolidated, in-depth analysis.

6 Summary and Conclusions

To summarise, the present study has two objectives. The first of these is to establish – or rather, emphasize – the fact that at a high energy e^+e^- collider, ISR and beamstrahlung can play a crucial role in the identification of new physics effects. This is a positive feature of these radiative phenomena, which is being now increasingly recognised as an important feature distinguishing such machines from low-energy colliders such as the LEP and its predecessors. The particle to be discovered can be of any kind, provided it is a neutral boson, as demanded by the total quantum numbers of the initial e^+e^- state. As our work is of illustrative nature, we have focussed on the cleanest final state, viz., $\mu^+\mu^-$, even though the other final states may also play a useful role. The second objective of our work is to apply this analysis to the case of massive graviton resonances. Earlier studies of such graviton resonances at e^+e^- colliders have assumed that the linear collider will run over a continuously-varying range of energies, which is almost certainly not going to be the case. We find that we are able to recover all the features of those earlier analyses simply by including radiation effects at a fixed machine energy. Not only do we find the resonant 'bumps', but we can also measure the spin of the resonant particle, even in the presence of large missing energy. This is achieved by the simple technique of reconstructing the 'boson' rest frame, a practice borrowed from the hadron collider toolkit.

If we consider the actual results obtained for the RS graviton search, it must be admitted that the results, except for those predicted at the CLIC, though useful enough, are not terrifically exciting. Since RS gravitons are already known to be heavier than 650 GeV, we have performed most of our analysis at the 800 GeV option of the TESLA, where the beam parameters are clearly enunciated, rather than at the 1 TeV option of the ILC, which is still at the planning stage. The actual kinematic range which can be probed is, therefore, already rather small, lying somewhere between 650 GeV and about 780 GeV. This cannot be helped, since the TESLA/ILC designs are intended for a different purpose, viz. precision measurements of physics that will be discovered (hopefully) at the LHC. At the CLIC, however – assuming that it will be built some day – we find that graviton searches take on an entirely different level of importance. In fact, for graviton searches, CLIC would far

surpass machines like the Tevatron, the TESLA/ILC, and may do significantly better than the LHC. Our results may, therefore, be considered a strong motivation to build a multi-TeV linear collider at some time in the not-so-remote future. Till then, we must be satisfied with the superior ability of linear colliders of lesser energy to make precision measurements of such attributes as the 'boson' spin. What is more to the point is that if graviton resonance(s) are lying just around the corner, as it were, then the LHC is likely to detect them, but identification of the resonances as gravitons may prove quite difficult. In such cases, it is a linear collider which we must turn to for the measurement of spin, and here graviton production will be almost completely dependent on radiation effects, as shown in the present work.

Acknowledgments: This work was partially supported by the Department of Science and Technology, India, under project number SP/S2/K-01/2000-II. The authors would also like to thank the organisers of the *Eighth Workshop on High Energy Physics Phenomenology (WHEPP-8)* at Mumbai, India (January 2004), where the idea for making the present study originated.

References

[1] J. A. Aguilar-Saavedra *et al.* [ECFA/DESY LC Physics Working Group], hep-ph/0106315; http://tesla.desy.de/tdr/

[2] K. Abe *et al.* [ACFA Linear Collider Working Group], hep-ph/0109166; T. Abe *et al.* [American Linear Collider Working Group], in *Proc. of the APS/DPF/DPB Summer Study on the Future of Particle Physics (Snowmass 2001)* ed. N. Graf, hep-ex/0106055–0106058;

[3] R. D. Heuer, Nucl. Phys. Proc. Suppl. **154**, 131 (2006).

[4] R. Blankenbecler and S. D. Drell, Phys. Rev. **D36** 277 (1987); Phys. Lett. **B197** 253 (1987). M. Bell and J. S. Bell, Part. Accel. **22**, 301 (1988).

[5] C. F. von Weizsacker, Z. Phys. **88**, 612 (1934). E. J. Williams, Phys. Rev. **45**, 729 (1934).

[6] K. Yokoya and P. Chen, Lect. Notes Phys. **400**, 415 (1992); SLAC report SLAC-PUB-4935 *Presented at IEEE Particle Accelerator Conf., Chicago, Ill., Mar 20-23, 1989*; M. Peskin, SLAC report SLAC-TN-04-032; D. V. Schroeder, SLAC report SLAC-0371; M. Jacob and T. T. Wu, Nucl. Phys. **B371**, 59 (1992).

[7] P. Chen, Phys. Rev. **D46**, 1186 (1992).

[8] M. Drees and R. M. Godbole, Phys. Rev. Lett. **67**, 1189 (1991).

[9] K. Grassie and P. N. Pandita, Phys. Rev. D **30**, 22 (1984); A. Datta, A.K. Datta and S. Raychaudhuri, Phys. Lett. **B349**, 113 (1995) and Eur. Phys. J. C **1**, 375 (1998); S. Ambrosanio *et al*, Nucl. Phys. B **478**, 46 (1996).

[10] C. H. Chen, M. Drees and J. F. Gunion, Phys. Rev. Lett. **76**, 2002 (1996), Erratum – *ibid.* **82**, 3192 (1999)

[11] S.K. Rai and S. Raychaudhuri, JHEP **0310**, 020 (2003); T. Buanes, E.W. Dvergsnes and P. Osland, Eur. Phys. J. **C35**, 555 (2004).

[12] L. Randall and R. Sundrum, Phys. Rev. Lett. **83**, 3370 (1999).

[13] E. Accomando *et al.* [CLIC Physics Working Group], hep-ph/0412251.

[14] N. K. Mondal *et al.*, Pramana **63**, 1331 (2004).

[15] A. Datta, K. Kong and K.T. Matchev, hep-ph/0508161; O. Cakir, hep-ph/0604183.

[16] M. Drees and R. M. Godbole, Z. Phys. **C59**, 591 (1993) and references therein.

[17] F. Bloch and A. Nordsieck, *Phys. Rev.* **52**, 54 (1937).

[18] E. A. Kuraev and V. S. Fadin, Sov. J. Nucl. Phys. **41**, 466 (1985) [Yad. Fiz. **41**, 733 (1985)]; O. Nicrosini and L. Trentadue, Phys. Lett. **B196**, 551 (1987).

[19] P. Chen, *Differential Luminosity Under Multiphoton Beamstrahlung,* SLAC report SLAC-PUB-5615 (July 1991).

[20] S. Rolli (CDF Collaboration), hep-ex/0305027.

[21] T. Han, J. D. Lykken and R. J. Zhang, Phys. Rev. **D59**, 105006 (1999); G. F. Giudice, R. Rattazzi and J. D. Wells, Nucl. Phys. **B544**, 3 (1999); H. Davoudiasl, J. L. Hewett and T. G. Rizzo, Phys. Rev. Lett. **84**, 2080 (2000).

[22] T.G. Rizzo, Phys. Rev. **D59**, 113004 (1999).

[23] B. Bhattacherjee and A. Kundu, Phys. Lett. **B627**, 137 (2005).

[24] D. Choudhury, S.K. Rai and S. Raychaudhuri, Phys. Rev. **D71**, 095009 (2005).

[25] S. Eidelman *et al.* [Particle Data Group], Phys. Lett. **B592**, 1 (2004).

[26] I. Antoniadis, Phys. Lett. **B246**, 377 (1990); T. Appelquist, H.-C. Cheng and B. Dobrescu, Phys. Rev. **D64**, 035002 (2001); H.-C. Cheng, K.T. Matchev and M. Schmaltz, Phys. Rev. D **66** 056006 (2002).